

# Analyses on Nonlinear Ultrasonic Imaging of Closed Cracks by Damped Double Node Model

減衰 2 重節点モデルを用いた閉口き裂の非線形超音波映像の解析

Yoshikazu Ohara<sup>1†</sup>, Yohei Shintaku<sup>1</sup>, Satoshi Horinouchi<sup>1</sup> Masako Ikeuchi<sup>1</sup> and Kazushi Yamanaka<sup>1</sup> (<sup>1</sup>Tohoku Univ.)

小原 良和<sup>1†</sup>, 新宅 洋平<sup>1</sup>, 堀之内 聡<sup>1</sup>, 池内 雅子<sup>1</sup>, 山中 一司<sup>1</sup> (<sup>1</sup>東北大)

## 1. Introduction

Nonlinear ultrasound is the most effective means in detecting closed cracks. Among them, the subharmonic wave attracts particular interest due to its high selectivity for closed cracks.<sup>1)</sup> Hence, we have developed a practical imaging method, subharmonic phased array for crack evaluation (SPACE).<sup>2-3)</sup>

For the application of the subharmonic waves and its scientific understanding, we extended 1D simple oscillator model<sup>1)</sup> to the 2D simulation based on finite difference time domain (FDTD) method with damped double node (DDN).<sup>4)</sup> We observed the vibration of crack faces and successfully reproduced subharmonic generation. However, it has yet to be applied to an imaging of closed crack based on the imaging algorithm of SPACE.

Here we extend the analyses to subharmonic imaging of closed cracks. The input-amplitude dependence of subharmonic response is examined. By utilizing the dependence, we simulate closed-crack imaging with high selectivity.

## 2. DDN model in FDTD method<sup>4)</sup>

In the 2D analysis, staggered grids are used for the calculation of particle velocities and stresses by the FDTD method. In **Fig. 1**,  $\dot{u}$  and  $\dot{w}$  are particle velocities in  $x$ - and  $z$ -directions,  $T_1 = T_{xx}$ ,  $T_3 = T_{zz}$  are the normal stresses, and  $T_5 = T_{xz}$  is the shear stress. The fundamental equations for isotropic elastic solids are Hooke's law and Newton's second law of motion. The calculation by the FDTD method follows the standard approach.<sup>5)</sup>

In the closed state, the crack faces are represented by normal nodes. In the open state, the normal nodes are split into double nodes consisting of the particle velocity of incidence-side crack face  $\dot{w}^-$  and particle velocity of transmission-side crack face  $\dot{w}^+$ . To simulate closed crack faces with compression residual stress, we introduced a viscous damping into the double node as shown by the dash pots. The transition between the open and closed state was described in ref. 4.

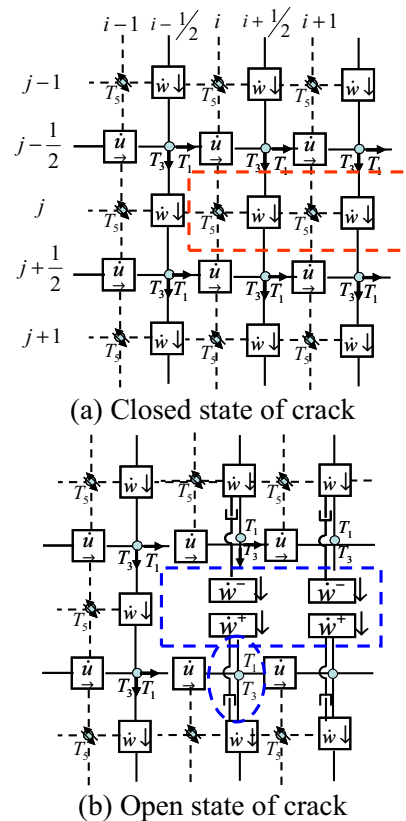


Fig. 1 DDN model in FDTD method.

## 3. Simulation model

Calculation was carried out with a time interval of 2 ns and node interval of 0.02 mm in models of **Fig. 2**. Plane waves of 3-cycles burst at frequency  $f = 8$  MHz was excited by a 32-element array at the surface. Residual compression stress was set to 100 MPa. The damping coefficient was set to 0.7 to suppress the noise.

## 4. Simulation results

We calculated fundamental array (FA) and subharmonic array (SA) images, by filtering the received waveforms at  $f$  and  $f/2$ , respectively. In 2D image of **Fig. 3 (a)** and SA image of **Fig. 4 (b)** at 40 nm input amplitude, there is no crack response. On the otherhand, there are scattered waves at the crack in 2D image of **Fig. 3 (b)** and SA image of **Fig. 5 (b)** at 120 nm input amplitude.

Then, we examined the intensity of crack and slit responses in SA images for input amplitudes from 10 nm to 120 nm (**Fig. 6**). The crack response was absent until 60 nm and it markedly increased at above 60 nm. This is the threshold behavior known in literatures of subharmonic generation.<sup>6)</sup>

It is noted the slit **S** and back surface **B** appeared in SA images although they are linear scattering sources. They are artifacts due to the leak of frequency filtering, degrading selectivity of closed crack imaging.

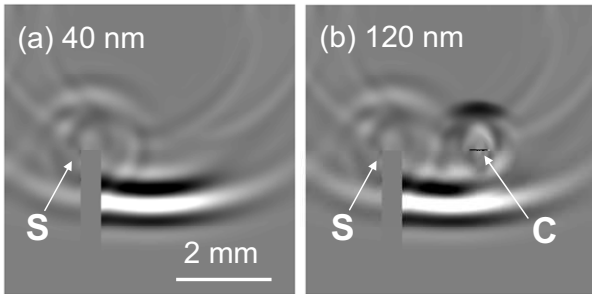
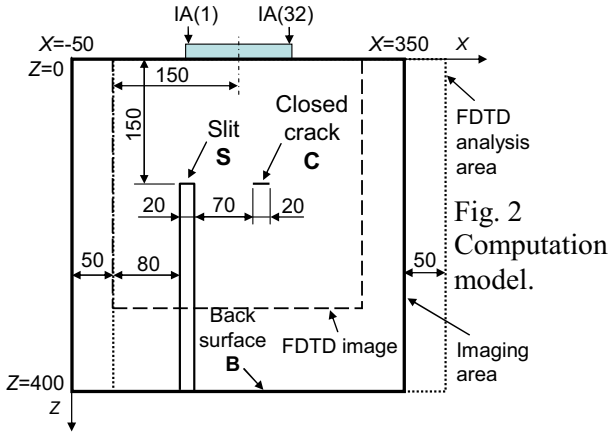


Fig. 3 FDTD images of scattered wave fields.

To eliminate the artifacts in SA image, we utilize the nonlinearity of crack response and the linearity of the artifact response in SA images against input amplitude. Then, we subtracted SA image (Fig. 4 (b)) at 40 nm input multiplied by an amplification factor  $a = 120 \text{ nm} / 40 \text{ nm} = 3$  from the SA image (Fig. 5 (b)) at 120 nm input. Then, we successfully eliminated the artifact of slit **S** and back surface **B**, and imaged only the closed crack **C**, as shown in **Fig. 7**. Assuming the selectivity is the intensity ratio of **C** to **B**,<sup>7)</sup> it was improved by 11.4 dB by canceling the artifact.

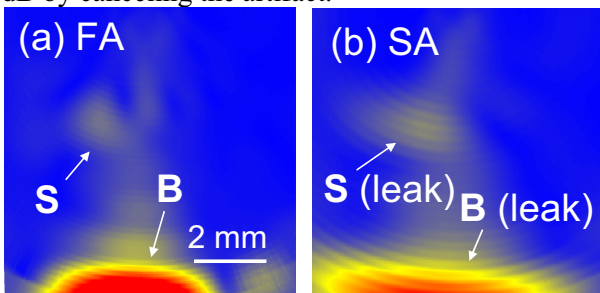


Fig. 4 FA and SA images at 40 nm input amplitude

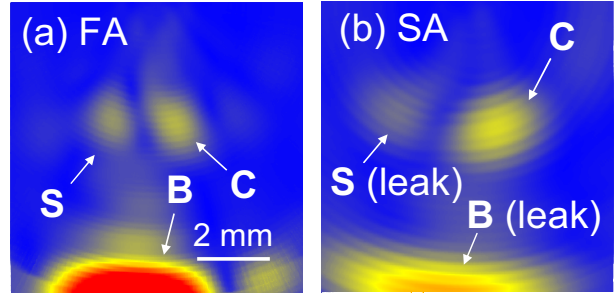


Fig. 5 FA and SA images at 120 nm input amplitude

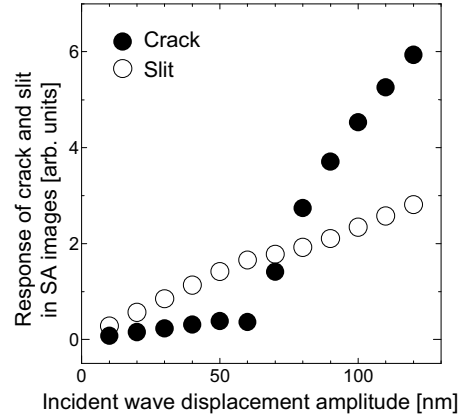


Fig. 6 Input wave amplitude dependence of responses in SA images.

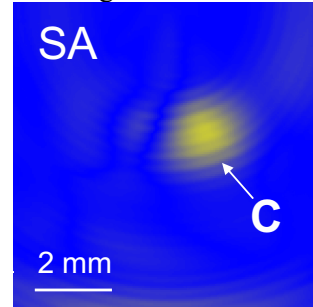


Fig. 7 Subharmonic image after artifact elimination.

This method will be generally useful not only in subharmonic but also in superharmonic imaging.

## 5. Conclusions

We extended the DDN simulation to subharmonic imaging of closed cracks. The input-amplitude dependence of subharmonic response was examined, and we succeeded in closed-crack imaging with high selectivity.

## Acknowledgment

This work was supported by Grants-in-Aid for Scientific Research (Nos. 21246105 and 21686069) from the Japan Society for the Promotion of Science.

## References

1. K. Yamanaka, et al.: JJAP. **43** (2004) 3082.
2. Y. Ohara, et al.: APL **90** (2007) 011902.
3. Y. Ohara, et al.: JJAP **48** (2009) 07GD01.
4. K. Yamanaka, et al.: APEX **4** (2011) 076601.
5. M. Sato: Acoust. Sci. Technol. **28** (2007) 49.
6. I. Y. Solodov, et al.: PRL **88** (2002) 014303.